"Kinetic polymer arrest in percolated SWNT networks"

Rana Ashkar,[†,*] Mansour Abdul Baki,[‡] Madhusudan Tyagi, [†,*] Antonio Faraone, [†,*] Paul Butler,[*,§] and Ramanan Krishnamoorti[‡]

[†]*Materials Science and Engineering Department, University of Maryland, College Park, MD 20742*

[*]*NIST Center for Neutron Research, Gaithersburg, MD 20899*

[‡]*Department of Chemical & Biomolecular Engineering, University of Houston, Houston, TX 77204*

[§]*Department of Chemical Engineering, University of Delaware, Newark, DE 19711*

I. Experimental

A. Sample Preparation[1].

In this work, we prepared two types of samples, fully deuterated atactic PMMA (dPMMA) samples for neutron diffraction and spin-echo measurements and protonated atactic PMMA samples for neutron backscattering measurements. The polymers were purchased from Pressure Chemical Co. with molecular weights, M_w (dPMMA) = 25 kg/mole and M_w (PMMA) = 254.7 kg/mole and a polydispersity index of 1.15. Both molecular weights are beyond the entanglement molecular weight (12.5 kg/mole) of atactic PMMA[2]. The nanotubes (purchased from Nano-C Inc.) were prepared by a combustion process and purified using an oxidative acid to remove metal contaminants.

The hydrogenated composites were prepared with SWNT volume fractions (1, 8, and 15) % and the deuterated composite with a SWNT volume fraction of 8 %. The reported concentrations are calculated from mass measurements using the following densities: $\rho_{\mathrm{SWNT}} = 1.62\ \mathrm{g/cm^3}$, $\rho_{\mathrm{hPMMA}} = 1.18\ \mathrm{g/cm^3}$ and $\rho_{\mathrm{dPMMA}} = 1.266\ \mathrm{g/cm^3}$. These SWNT concentrations are well beyond

the structural percolation threshold of well dispersed slender rod-like objects[3]. The nanotubes were dispersed in dimethylformamide (DMF) by sonicating dilute dispersions for 30 minutes in a low-power water-cooled sonicator. The polymer was dissolved separately in DMF using a rotary stir bar for 24 hours. The dispersion of SWNTs was added to the stirring polymer solution and allowed to mix for ≈ 24 hours. The nanocomposite was recovered by a non-solvent extraction (coagulation) method as outlined previously by Du *et al*[4].

For neutron scattering experiments, the samples were solvent cast onto petri dishes and then transferred to aluminum boats that were wrapped into annular cylinders to fit in an aluminum sample canister which is typical for such measurements. The samples were transferred to the sample container inside a helium glove box and sealed with lead. The enclosed helium ensures excellent heat transfer and minimizes temperature gradients during the measurements.

B. Neutron Scattering Measurements

Neutron diffraction was used to characterize local chain ordering in pure and composite PMMA, neutron backscattering to track atomic motions at different SWNT loadings, and neutron spin-echo (NSE) spectroscopy to probe the effect of SWNT percolation on the chain relaxations. Backscattering measurements were performed at the High Flux Backscattering Spectrometer (HFBS) on the NG2 beam line at the NIST Center for Neutron Research (NCNR). Diffraction and NSE data were collected at the NSE spectrometer on the NG5 beam line at NCNR. The data reduction was done using the Data Analysis and Visualization Environment (DAVE) software[5] developed by NIST.

1. Neutron Diffraction and Neutron Spin Echo. Neutron diffraction and spin-echo experiments were performed on fully deuterated samples in order to minimize the incoherent signal that

constitutes the background in such measurements. Neutron spin echo (NSE), in particular, yields the normalized intermediate scattering function:

$$\frac{\mathrm{S}(Q,t)}{\mathrm{S}(Q,0)} = \frac{I(Q,t)}{I(Q,0)} \qquad \text{(I)}$$

The momentum transfer, Q, and the time parameter, t, in expression (I) respectively set the length and time scales over which the dynamics are probed. The time parameter is given by $t \propto \lambda^3$ and the magnitude of Q by $Q = 4\pi \sin(\theta/2)/\lambda$ where λ is the wavelength of the incident neutron beam and θ is the corresponding scattering angle. NSE measurements were performed at a Q value of 0.9 Å^{-1}, with λ = 6 Å and wavelength spread of $\Delta\lambda/\lambda \approx 20$ %, covering a time range of 7 ps to 15 ns.

2. Neutron Backscattering. Backscattering measurements were carried out on the fully protonated pure and composite PMMA samples. The samples were prepared with a thickness of (0.1 to 0.2) mm in order to minimize the contribution of multiple scattering and ensure ~ 90% transmission. In these samples, the incoherent scattering cross-section of hydrogen is about an order of magnitude greater than its coherent counterpart and the total cross-section of carbon and oxygen. The signal is, thus, dominated by incoherent scattering from the hydrogenated polymer matrix and the measured dynamics are solely those of the polymer. The HFBS spectrometer was operated in elastic or fixed-window scan (FWS) mode, and the incoherent elastic intensities, I_{el}^{inc}, were recorded over a Q-range of (0.25 to 1.75) Å^{-1} for temperatures between 50 K and 460 K at a heating rate of 1 K/min. The Q-dependence of I_{el}^{inc} was used to extract the mean-square displacements (MSD) of the hydrogen atoms within the samples.

II. Data analysis and discussion

1. Backscattering measurements: MSD calculations

Elastic incoherent intensities, $I_{el}^{inc}(Q,T)$, were collected over all of the 16 detectors of the HFBS instrument for each sample over a wide range of temperatures. The amplitude, $<u^2>$, of the mean-square-displacements is calculated from the *Q*-dependence of the intensities collected over each detector using the Debye-Waller approximation:

$$\ln\left[I_{el}^{inc}(Q,T)\right] = -\frac{1}{3}Q^2 <u^2(T)> \qquad \text{(II)}$$

Despite being based on rather crude approximations, equation (II) is widely employed in the analysis of backscattering data and has been shown to correctly identify the temperatures at which specific dynamical processes activate[6]. However, this expression dictates that the fits should intercept the intensity axis at the origin. Our data do not follow this pattern (see Figure S1), an observation that has been previously reported on similar systems[7,8] and was recently revisited in a theoretical study[9] which addresses possible shifts in the data due to coherent and multiple scattering effects. In such cases, equation (II) is modified to include a *T*-dependent intercept for the intensity, *C*(*T*), such that:

$$\ln\left[I_{el}(Q,T)\right] = -\frac{1}{3}Q^2 <u^2(T)> + C(T) \qquad \text{(III)}$$

Equation (III) gives a good description of our data as shown in Figure S1, with the exception of some deviations at low-*Q* which are attributed to rotational reorientation of the methyl side groups[7]. As far as the MSDs are concerned, the actual extracted value should be considered to be only qualitative in the absence of a detailed model of the scattering function. In this scheme, the comparison of two analog systems, PMMA and its composites, can be carried out with confidence. The MSDs obtained from the fits are presented in Figure 1b in the manuscript.

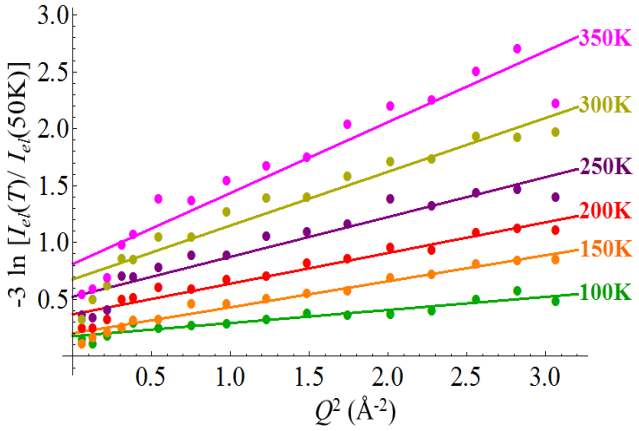

Figure S1. Sample of the I_{el}^{inc} data on PMMA presented as a function of Q^2. The straight lines are fits to the data according to equation (III). The slopes determine the mean square displacement amplitudes, $<u^2>$, of the hydrogen atoms in the polymer matrix. Error bars are omitted for clarity.

2. Neutron diffraction

The Q-range associated with the targeted dynamics was determined using neutron diffraction prior to NSE measurements. The static structure factors of dPMMA and its nanocomposite with 8 % volume fraction SWNTs (Figure S2) show the main diffraction peak[10] at $Q \approx 0.9$ Å^{-1}, which is characteristic of nearest neighbor spacing. The average nearest-neighbor distance is found from the peak position to be ≈ 7 Å. When the samples are heated, the peak position moves slowly towards slightly lower Q values, as expected.

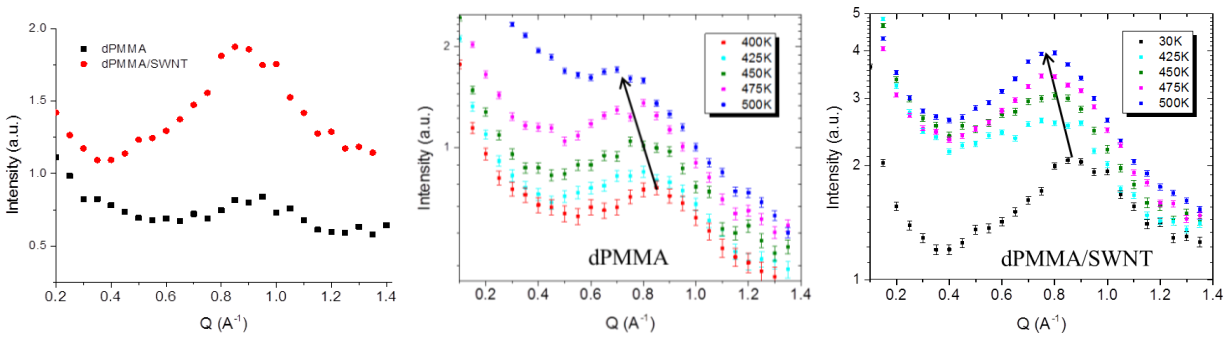

Figure S2. (a) Neutron diffraction patterns of dPMMA and its composite with 8 % SWNTs at T = 30K shifted vertically for clarity. The peak around Q =0.9 Å^{-1} indicates inter-chain separation. (b) and (c) Evolution of the diffraction patterns upon heating showing a gradual shift in the peak position towards smaller Q values with increasing temperatures.

3. Neutron Spin Echo

Since the chain relaxations of the polymer matrix occur at length scales comparable to the intra-chain spacing, the NSE instrument was tuned to selectively probe dynamics at the peak position in Figure S2, *i.e.* $Q = 0.9$ Å^{-1}. The intermediate scattering functions of dPMMA and the dPMMA composite with 8 % SWNT loading in Figure S3 show that the decay is very slow at low temperatures (close to T_g) but it gets faster at higher temperatures as the chains gain enough thermal energy. The decay is described by a stretched exponential behavior, $\exp[-(t/\tau_R)^{\beta}]$, typical of polymeric systems[11,12]. The deviation from unity of the decay amplitudes in NSE data are usually attributed to fast dynamical processes with decay times (few picoseconds or smaller) that are beyond the temporal sensitivity of the NSE technique[10]. In the NSE window, this is usually accounted for by a scaling factor, referred to as an effective Debye-Waller Factor, *DWF*. A proper description of the dynamic structure factor is then given by a modified stretched exponential of the form:

$$\frac{S(Q,t)}{S(Q,0)} = DWF \exp\left[-\left(\frac{t}{\tau_R}\right)^{\beta}\right] \qquad \text{(IV)}$$

where τ_R is the temperature-dependent relaxation time of the polymer chains. Equation (IV) is also known as the Kohlrausch-Williams-Watts (KWW) function. The parameters τ_R, β, and *DWF* are obtained from fits of expression (IV) to the NSE data sets of each sample for all the studied temperatures. It is important to realize that τ_R and *DWF* are temperature dependent, whereas the stretching exponent β is, in principle, independent of temperature. In the course of fitting, the value of β was extracted from the high-T data set that shows the most pronounced decay and was used as an initial value for the fits of the lower-T data sets. An iterative approach was adopted until the β-parameter from all T-sets on a given sample converged to within 15 %.

This step is necessary for a reliable extraction of τ_R and a proper description of the relaxation dynamics. The resultant β-values were found to be 0.71 ± 0.13 and 0.52 ± 0.09 for dPMMA and dPMMA/SWNT, respectively (Figure S3). The β-value obtained for dPMMA is somewhat larger than the 0.5 value commonly observed in polymer systems, although we are not the first to report such value[12-14]. From a theoretical standpoint, β describes the distribution of decays of individually relaxing species within the sample[15]; values of β close to zero indicate lack of decay over the measurement time whereas β-values approaching unity correspond to a single decay mode. The stronger deviation from unity of the β-value for the composite is then an indication of increased dynamical heterogeneities in the composite, which is consistent with the discussion on the coexistence of fast and slow polymer domains in the composite.

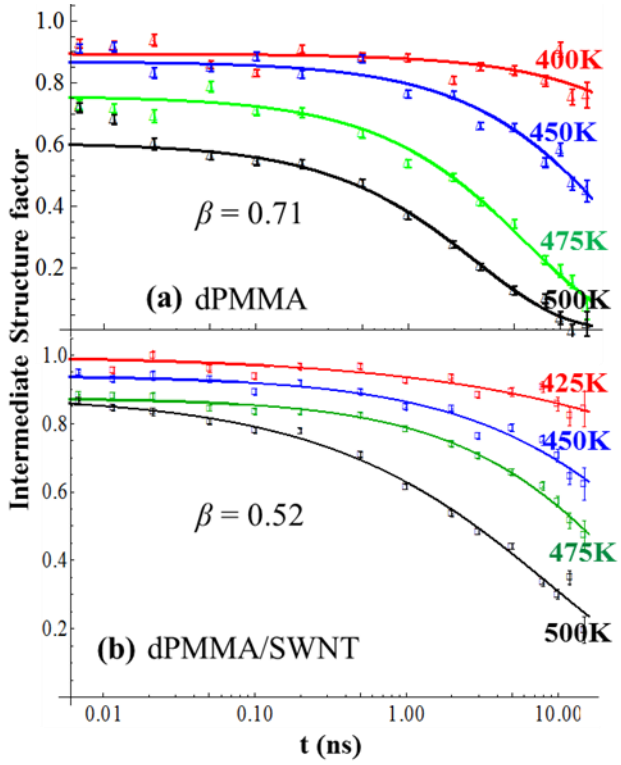

Figure S3. (a) NSE scans on dPMMA as a function of temperature along with the KWW fits (solid lines) performed with a stretching exponent β = 0.71 ± 0.13. **(b)** The dynamic structure factor obtained by NSE on the composite with a SWNT volume fraction of 8 % for different temperatures. The solid lines are KWW fits with β = 0.52 ± 0.09.

III. TEM characterization of the SWNT network

The dispersion of the nanotubes within the composites was investigated by transmission electron microscopy (TEM) on microtomed slabs of the samples. The TEM images show that the nanotubes form networks of few-nm-diameter aggregates or bundles. A sample of the images on the deuterated composite with 8 % volume fraction SWNTs is shown in Figure S4. Image analysis of several such micrographs was used to get the average aggregate diameter. For the sample shown here, the average diameter is found to be ≈ 8 nm.

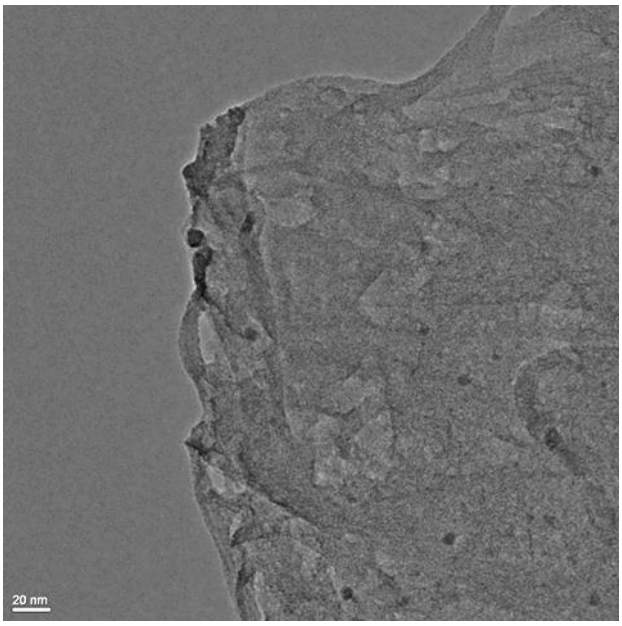

Figure S4. TEM image of a microtomed section of the dPMMA composite with 8 % volume fraction SWNTs. The image shows a network of nanotube aggregates with an average diameter of ≈ 8nm.

References

(1) *The identification of any commercial product or trade name does not imply endorsement or recommendation by the National Institute of Standards and Technology.*

(2) Krishnamoorti, R.; Graessley, W. W.; Zirkel, A.; Richter, D.; Hadjichristidis, N.; Fetters, L. J.; Lohse, D. J. *Journal of Polymer Science Part B: Polymer Physics* **2002**, *40*, 1768.

(3) Bug, A. L. R.; Safran, S. A.; Webman, I. *Physical Review Letters* **1985**, *54*, 1412.

(4) Du, F.; Scogna, R. C.; Zhou, W.; Brand, S.; Fischer, J. E.; Winey, K. I. *Macromolecules* **2004**, *37*, 9048.

(5) Azuah, R. T.; Kneller, L. R.; Qiu, Y.; Tregenna-Piggott, P. L.; Brown, C. M.; Copley, J. R.; Dimeo, R. M. *Journal of Research of the National Institute of Standards and Technology* **2009**, *114*, 341.

(6) Chahid, A.; Alegria, A.; Colmenero, J. *Macromolecules* **1994**, *27*, 3282.

(7) Frick, B.; Fetters, L. J. *Macromolecules* **1994**, *27*, 974.

(8) Alejandro, S.; Markus, R.; Jack, F. D.; João, T. C. *Journal of Physics: Condensed Matter* **2008**, *20*, 104209.

(9) Zorn, R. *Nuclear Instruments and Methods in Physics Research Section A: Accelerators, Spectrometers, Detectors and Associated Equipment* **2007**, *572*, 874.

(10) Frick, B.; Richter, D. *Science* **1995**, *267*, 1939.

(11) Genix, A. C.; Arbe, A.; Alvarez, F.; Colmenero, J.; Schweika, W.; Richter, D. *Macromolecules* **2006**, *39*, 3947.

(12) Tyagi, M.; Alegría, A.; Colmenero, J. *The Journal of Chemical Physics* **2005**, *122*.

(13) Tyagi, M.; Arbe, A.; Colmenero, J.; Frick, B.; Stewart, J. R. *Macromolecules* **2006**, *39*, 3007.

(14) Pérez-Aparicio, R.; Alvarez, F.; Arbe, A.; Willner, L.; Richter, D.; Falus, P.; Colmenero, J. *Macromolecules* **2011**, *44*, 3129.

(15) Palmer, R. G.; Stein, D. L.; Abrahams, E.; Anderson, P. W. *Physical Review Letters* **1984**, *53*, 958.